Electron g-factor anisotropy in GaAs/$Al_{1-x}Ga_xAs$ quantum wells of different symmetry

Yu. A. Nefyodov,[1,*] A. V. Shchepetilnikov,[1] I. V. Kukushkin,[1] W. Dietsche,[2] and S. Schmult[2]
[1]*Institute of Solid State Physics RAS, 142432 Chernogolovka, Moscow District, Russia*
[2]*Max-Planck-Institut für Festkörperforschung, Heisenbergstr. 1, D-70569 Stuttgart, Germany*
(Received 6 October 2011; revised manuscript received 22 November 2011; published 8 December 2011)

The anisotropy of the electron g factor is investigated in symmetrically (SQW) and asymmetrically (AQW) doped 20-nm GaAs/AlGaAs quantum wells, grown in the [001] direction. Applied was the electrically detected electron spin resonance technique. The AQW demonstrates strong twofold in-plane g-factor anisotropy with the [110] and [1$\bar{1}$0] principal axes. This can be readily ascribed to the internal electric field asymmetry as caused by single-side doping. The SQW is shown to have 10 times as weak (but still detectable) anisotropy with the same principal axes. The linear (in the magnetic field) corrections to the g factor were also carefully measured. The $\hat{a}$ tensor of these corrections is shown to have at least three different nonzero components, namely, a_{zzz}, a_{xxz}, and a_{yyz}.

DOI: 10.1103/PhysRevB.84.233302 PACS number(s): 73.43.Lp, 73.43.Qt, 76.30.−v

Spin phenomena in two-dimensional (2D) systems are of great fundamental and applied interest. The fundamental one includes such effects as metal-insulator transition,[1] excitonic effects,[2] spin Hall effect,[3] etc. With comprehensive knowledge of all factors that affect spin splitting, one can successfully manipulate spin states. This provides the opportunity of making ultimately small logical elements and memory arrays with a high operational frequency, low energy consumption, and high informational capacity.[4]

Spin phenomena are commonly described by the Landé g factor, which again is determined by spin-orbit interaction. In bulk zinc-blende materials with T_d point group symmetry the g factor is reduced to a scalar. In the case of two-dimensional systems, the situation changes due to the symmetry reduction. This reduction is strongly dependent on the quantum well growth direction. The most symmetric wells are those grown in the [001] direction. It is such wells we investigated in the present paper. If the intrinsic electric field potential is symmetrical in the growth direction, the point group symmetry of the well is D_{2d}, and the electron g factor is isotropic in the well plane; that is, the $g_{\alpha\beta}$ tensor has only two independent components, namely, $g_\perp \neq g_\parallel$. The asymmetry of the potential leads to the point group symmetry reduction to C_{2v}, giving rise to the in-plane g-factor anisotropy. Thus, in the principal axes, the $g_{\alpha\beta}$ tensor should have three independent components g_{xx}, g_{yy}, g_{zz}. This fact was theoretically predicted in Ref. 5 and was observed experimentally in undoped quantum wells.[6,7]

The present paper aims to carefully investigate the in-plane and out-of-plane anisotropy of the g factor in doped GaAs/AlGaAs quantum wells grown in the [001] direction, to determine experimentally the influence of the quantum well symmetry on this anisotropy, and to estimate the values of the $\hat{a}$ tensor of the linear in the magnetic field correction to the g factor.

Following Ref. 5, consider a 2D quantum well of the finite width (Oz axis is parallel to the growth direction) in the magnetic field **B**. The magnetic field component parallel to [100] deflects the electron motion from the Oz axis, giving rise to small electron momentum alteration along [010], δp. The rise of this admixture changes the effective Rashba and Dresselhaus fields, defining the electron precession. The appropriate precession vectors are as follows:

$$\mathbf{\Omega}_R(\mathbf{p}) = \alpha/\hbar^2 \begin{pmatrix} p_\zeta \\ -p_\xi \\ 0 \end{pmatrix}, \quad \mathbf{\Omega}_D(\mathbf{p}) = \beta/\hbar^2 \begin{pmatrix} -p_\xi \\ p_\zeta \\ 0 \end{pmatrix}. \quad (1)$$

Here, the ξ,ζ axes coincide with the [100],[010] directions, respectively. The change in p_ζ due to the finite B_ξ yields an admixture in $\mathbf{\Omega}_R$, directed along ξ, which, hence, changes diagonal g-factor tensor components. $\mathbf{\Omega}_D$ gives rise to nondiagonal components $g_{\xi\zeta}, g_{\zeta\xi}$. Careful analysis[5] yields the following formulas:

$$g_{\xi\zeta} = g_{\zeta\xi} = \frac{2\gamma e}{\hbar^3 \mu_B}\left(\langle p_z^2\rangle\langle z\rangle - \langle p_z^2 z\rangle\right), \quad (2)$$

where γ is the Dresselhaus coefficient, μ_B is the Bohr magneton, and the averaging is done through the electron states in the quantum well. Since $g_{\xi\zeta} = g_{\zeta\xi}, g_{\xi\xi} = g_{\zeta\zeta}$, the directions [110], [1$\bar{1}$0], [001] should be the principal axes of $\hat{g}$. From Eq. (2) one can easily see that the in-plane g-factor anisotropy is defined by the wave-function symmetry along the growth direction and, hence, the symmetry of the intrinsic electric field potential. Aiming to simplify the experimental data discussion, we rotate reference axes around the [001] direction by 45° and define new axes $Ox \parallel [110]$ and $Oy \parallel [1\bar{1}0]$.

The investigations of the g factor in the 2D system have been performed earlier with the aid of Kerr rotation, quantum beat spectroscopy, and electrically detected electron spin resonance techniques. Optical techniques[10,11] were mainly used to study undoped quantum wells. Several theoretical papers[8,9] were devoted to the calculation of the g-factor tensor in such wells. In contrast, in the present paper undoped quantum wells are under investigation. It is worth noting that it is this type of well that is potentially suitable for spintronic applications. The electrically detected ESR technique was successfully used to study doped quantum wells.[12–16] In our previous paper,[13] we applied this technique to study a single-side doped 25-nm quantum well and showed strong anisotropy of $g_{\alpha\beta}$ in such a system.

The conventional ESR technique cannot be successfully applied to 2D electron systems[17] due to the low number of

spins. However, as early as 1983, magnetoresistance of the 2DEG was shown[15] to be very sensitive to spin resonance when the Fermi level is located between spin-split states of a given Landau level. Having measured the fraction $\delta\rho_{xx}$ of the magnetoresistance ρ_{xx}, arising due to the RF quantum absorbtion, it is possible to observe spin resonance as a peak in $\rho_{xx}(B)$ at a fixed RF frequency.

In the ESR experiment, the electron from the lower spin state absorbs the RF energy quantum and is excited to a higher state. This spin-flip transition is accompanied by the appearance of the hole in the lower spin state. The excited electron and the hole form the bounded state–spin exciton. The dispersion relation of spin waves at finite wave vectors was calculated in Ref. 2. Since the RF power wave vectors are much smaller than the reciprocal magnetic length, the excitonic effects do not significantly affect spin splitting and thus, the experimentally measured g factor corresponds to zero wave-vector limit.

Two $Al_xGa_{1-x}As/GaAs$ quantum wells of equal 20-nm widths were studied. Both of them were grown in the [001] direction using the MBE technique. Sample No. 1 (AQW) is a single side delta-silicon doped well with 2DEG density $n \approx 4.4 \times 10^{11}\,\mathrm{cm}^{-2}$, whereas the mobility amounted to $6 \times 10^5 \frac{V}{\mathrm{cm}^2\mathrm{s}}$ at liquid-helium temperature. The sample No. 2 (SQW) is a symmetrical, two-side doped well with electron density $n \approx 4.8 \times 10^{11}\mathrm{cm}^{-2}$ and the mobility $4.5 \times 10^5 \frac{V}{\mathrm{cm}^2\mathrm{s}}$. Usual Hall bar mesas were prepared on both samples. In Ref. 13 we showed that the g factor does not depend on the orientation of the mesa and, hence, the direction of the probe current with respect to crystal axes, but it does depend on the magnetic field orientation.

An ac probe current of 1 μA at the frequency of $\sim$1 kHz was applied from source to drain. A lock-in amplifier monitored the channel resistance R_{xx} through two sense contacts along the channel. The sample was illuminated by 100% amplitude modulated radiation at the frequency of f_{mod} $\sim$30 Hz; RF power was delivered from an Anritsu MG3696B generator through a rectangular waveguide. A second lock-in amplifier, synchronized at the frequency of f_{mod}, was connected to the output of the first one and thus measured the change δR_{xx} in the magnetoresistance, caused by microwave irradiation.

It is common knowledge that hyperfine interaction of electron and nuclear spins can cause dynamic polarization of nuclear spins, which results in shifting of the position and changing of the shape of the ESR line.[16,18] The more the RF power, the more pronounced is the effect, which was successfully used to study nuclear spin relaxation rates.[16] In our experiments, we used so low RF power that the influence of dynamic polarization was negligible, that is, the ESR line shape and position did not change with RF-power variations. The actual RF-power incident to the sample amounted to $\lesssim$1 mW. Experiments were carried out at the temperatures of $1.3 \div 4.2$ K in the magnetic fields up to 10 T. In our experiments, we fixed the microwave frequency and swept the magnetic field. In Ref. 12, we showed that the results of ESR measurements using the frequency and magnetic field sweeps do coincide, but the magnetic field sweep is much more convenient in the experiment.

The ESR signal was observed in the vicinity of filling factors $\nu = 3,5,7$ with the linewidth amounting to $\sim$20 mT in these samples. The ESR linewidth was found to be dependent on the magnetic field strengths and orientation. This phenomenon will be discussed in detail elsewhere.

To study the g-factor anisotropy, we mounted the sample on the rotation stage in such a manner that the normal to the 2DEG plane formed an angle θ with the magnetic field B, whereas the sample axis x formed an angle ϕ with the in-plane magnetic field component. Both angles θ and ϕ can be easily changed and measured with the aid of a three-dimensional (3D) magnetic field sensor rigidly attached to the sample. The value of θ is double-checked by the 3D magnetic field sensor and by the measurements of the Hall voltage on the sample under investigation. Assuming the axes x,y,z to be the principal ones, we expect the following formula to be valid:

$$g_0^2(\theta,\phi) = \left[g_{xx}^2 \cos^2\phi + g_{yy}^2 \sin^2\phi\right] \sin^2\theta + g_{zz}^2 \cos^2\theta, \quad (3)$$

where g_{xx}, g_{yy}, g_{zz} are the principal values of the g-factor tensor.

With the angles θ,ϕ fixed, we measure the ESR resonance magnetic field $B_{\mathrm{ESR}} = \frac{B_{\mathrm{up}}+B_{\mathrm{down}}}{2}$ for successive set of microwave irradiation frequencies f. Here, B_{up} and B_{down} are the spin resonance magnetic fields for upward and downward field sweeps, respectively. All thus obtained dependencies $f(B_{\mathrm{ESR}})$ can be perfectly fitted near the odd filling factors by parabolic expression $f = f_0 + \mu_B B(g + aB)$ with negligible f_0. The dependence $g(B) = \frac{hf}{\mu_B B}$ is piecewise linear with discontinuities at even filling factors.[19] The linear $g(B)_{B\to 0}$ extrapolations of continuous near different odd filling factor sections give the same value of the g factor at zero magnetic field.[13] Hence, the effective g factor near the subband bottom can be easily obtained by the linear extrapolation $g_0(\theta,\phi) = \lim_{B\to 0} g(\theta,\phi,B) = \lim_{B\to 0} \frac{hf}{\mu_B B}$ of any continuous section. In our experiments we used the sections near the filling factor $\nu = 3$. Furthermore, the linear term aB of this extrapolation can be used to estimate the values of the tensor $a_{\alpha\beta\gamma} = \frac{\delta g_{\alpha\beta}}{\delta B_\gamma}$. In the perpendicular magnetic field the coefficient a is dependent on the Landau level number N: $a = \mathrm{const}(N + \frac{1}{2})$, the fact predicted theoretically[19] and established experimentally.[13,14]

During the first set of the experiments, we fixed the angle ϕ to zero or 90° and measured the effective g factor for three successive θ values from zero [this gives us directly $g_{zz} \equiv g(\theta = 0,\phi)$] to $\approx$45°. According to Eq. (3), the extrapolations of g_0^2 to $\cos^2\theta = 0$ give us the values g_{xx}, g_{yy}. This is illustrated in Fig. 1, where the experimental points for AQW and SQW are shown by circles and squares, respectively; the data for $\phi = 0$ and 90° are shown by solid and open symbols. The result of fitting the data on Fig. 1 for AQW gives significantly different $|g_{xx}| = 0.292$ and $|g_{yy}| = 0.349$, which are very close to those obtained earlier[13] for 25-nm wide AQW. This fact is due to the saturation of the g factor with increasing well width.[8] In the case of SQW, the in-plane components appeared to be equal $|g_{xx}| = |g_{yy}| = 0.340$ within the experimental uncertainty.

To resolve the in-plane g-factor anisotropy more precisely, we performed another set of the experiments. We fixed the angle $\theta = 45°$ and changed the angle ϕ successively. The rotation was performed *in situ*, that is, without thermocycling. Knowing

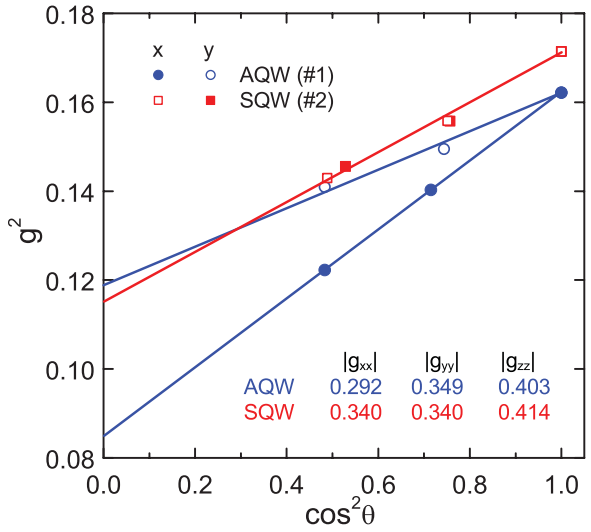

FIG. 1. (Color online) The dependencies of the effective g factor squared on the $\cos^2\theta$. The experimental points for AQW and SQW are shown by circles and squares, respectively; the data for $\phi = 0$ and 90° are shown by solid and open symbols. The intersection of solid lines with vertical axis give us g_{xx} and g_{yy} according to Eq. (3).

the value of $|g_{zz}|$ from the experiments at $\theta = 0$ and using Eq. (3) again in the similar manner, we get the in-plane g-factor anisotropy $g_{\parallel}(\phi) \equiv g(\theta = 90^\circ, \phi) = \sqrt{2g^2(\theta = 45^\circ, \phi) - g_{zz}^2}$, as shown in Fig. 2. The result of fitting (solid line) the data for AQW in Fig. 2 clearly shows the axes x and y to be the principal ones. Surprisingly, the SQW demonstrates behavior quite similar to AQW but with in-plane anisotropy 10 times as weak. Since the in-plane anisotropy is prohibited for a perfectly symmetric quantum well, a small remanent asymmetry of two-side doping of the sample under investigation could be a possible explanation of this phenomenon. The experimentally extracted principal values of $\hat{g}$ are shown in Table I. The g-factor sign is of common knowledge and was not extracted

TABLE I. The experimentally extracted values of $\hat{g}$ components ($Ox \parallel [110]$, $Oy \parallel [1\bar{1}0]$, and $Oz \parallel [001]$).

	AQW (No. 1)	SQW(No. 2)
g_{xx}	-0.292 ± 0.005	-0.343 ± 0.004
g_{yy}	-0.347 ± 0.005	-0.350 ± 0.004
g_{zz}	-0.403 ± 0.001	-0.414 ± 0.001

directly from the experiment. Slightly different values of g_{yy} appearing in Table I and in the table in Fig. 1 for the case of SQW can be caused by the change of electron density in the sample, which occurred because of thermocycling during the first set of experiments.

Let us discuss the possibility of estimating the components of the tensor of linear (in the magnetic field) corrections to the g factor: $\hat{a} = a_{\alpha\beta\gamma} = \frac{\delta g_{\alpha\beta}}{\delta B_\gamma}$ using the experimentally measured (at different magnetic field orientations) values of

$$a^* \equiv \frac{dg^*}{dB} = \frac{1}{g*} \sum_{i,j,k} g_{ij} a_{ijk} n_i n_j n_k, \tag{4}$$

where the quadratic in the magnetic field terms are omitted and

$$n_x = \sin\theta\cos\phi, n_y = \sin\theta\sin\phi, n_z = \cos\theta \tag{5}$$

are the fractions B_i/B of the total magnetic field B along the appropriate axis. Note that theoretically,[19] the only component of tensor $\hat{a}$, namely, a_{zzz}, should be nonzero. It can be directly measured in the perpendicular magnetic field: $g_{zz}(B) = g_{zz}(0) + a_{zzz}B$. Leaving only this term in Eq. (4),

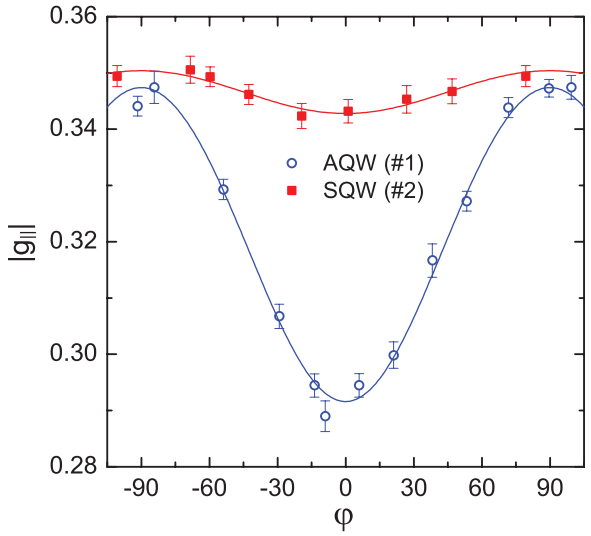

FIG. 2. (Color online) The experimental dependencies of the in-plane g factor on the angle ϕ. Open circles and solid squares stand for AQW and SQW, respectively. Solid lines show fits utilizing g_{xx} and g_{yy} as free parameters according to Eq. (3).

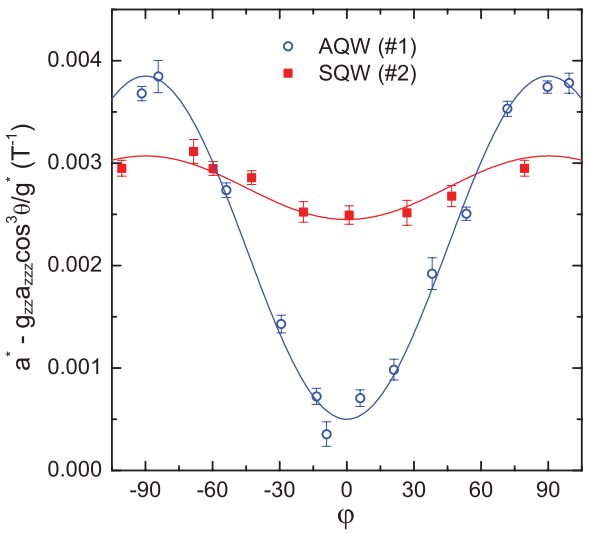

FIG. 3. (Color online) The dependencies of the linear (in the magnetic field) correction to the in-plane g factor on the angle ϕ, the independent on ϕ term due to a_{zzz} is subtracted. Lines show the fits using off-diagonal a_{xxz} and a_{yyz} terms indicated in Table II.

TABLE II. The experimentally extracted near the filling factor $\nu = 3$ values of $\hat{a}$ components ($Ox \parallel [110]$, $Oy \parallel [1\bar{1}0]$, and $Oz \parallel [001]$).

	AQW (T^{-1})	SQW (T^{-1})
a_{xxz}	0.002 ± 0.001	0.0075 ± 0.0005
a_{yyz}	0.012 ± 0.001	0.0090 ± 0.0005
a_{zzz}	0.017 ± 0.0001	0.016 ± 0.0001

we get the simplified formula for arbitrary angles:

$$a^* = \frac{g_{zz}a_{zzz}n_z^3}{g^*} = \frac{g_{zz}a_{zzz}}{g^*}\cos^3\theta, \tag{6}$$

which is independent on ϕ. In Fig. 3, we plot the experimental values of $a^* - \frac{g_{zz}a_{zzz}}{g^*}\cos^3\theta$ as a function of ϕ. Surprisingly, these dependencies are nonzero, as follows from Eq. (6), both for AQW and SQW, and clearly exhibit twofold symmetry on ϕ [as in the case of $g(\phi)$, the anisotropy of a^* is significantly weaker in the case of SQW]. This means the presence in $\hat{a}$ of some nonzero components in addition to a_{zzz}. Since $g_{ij} = 0$ for $i \neq j$, only $g_{ii}a_{iik}n_i^2n_k$ terms make a contribution to a^*. Moreover, as follows from Eqs. (4) and (5), only two of such terms, namely $g_{xx}a_{xxz}n_x^2n_z$ and $g_{yy}a_{yyz}n_y^2n_z$, give rise to the observed twofold symmetry of a^*. The lines in Fig. 3 show the experimental data fits using the off-diagonal a_{xxz} and a_{yyz} terms. Finally, Eq. (4) is reduced to the following form:

$$a^* = \frac{1}{g*}\sum_i g_{ii}a_{iiz}n_i^2n_z = \frac{1}{g^*}(g_{zz}a_{zzz}\cos^3\theta + [g_{xx}a_{xxz}\cos^2\phi + g_{yy}a_{yyz}\sin^2\phi]\sin^2\theta\cos\theta). \tag{7}$$

This means that all the principal values of the g-factor tensor are affected by the quantizing magnetic field through the change of band structure. In Table II we show the experimentally extracted values of $\hat{a}$ components. Note that despite the positive sign of these components, they reduce the g-factor absolute value due to the negative sign of the g factor itself.

In conclusion, we have carefully investigated the anisotropy of the electron g factor in symmetrically and asymmetrically-doped GaAs/AlGaAs quantum wells of 20-nm widths grown in the [001] direction. The $[110],[1\bar{1}0],[001]$ crystallographic directions were shown to be the principal axes of $\hat{g}$. The symmetry of the intrinsic electric-field potential of the structures investigated is shown to be mainly responsible for the in-plane g-factor anisotropy. The components of the $\hat{a}$ tensor of the linear (in the magnetic field) corrections to the g-factor tensor have also been investigated. The experimental data suggest the presence of nondiagonal $\hat{a}$ tensor components, namely, a_{xxz} and a_{yyz}, and allow us to estimate their values.

The research was supported by Russian Foundation for Basic Research.

*nefyodov@issp.ac.ru

[1] J. Yoon, C. C. Li, D. Shahar, D. C. Tsui, and M. Shayegan, Phys. Rev. Lett. **84**, 4421 (2000).
[2] C. Kallin and B. I. Halperin, Phys. Rev. B **30**, 5655 (1984).
[3] Y. K. Kato, R. C. Myers, A. C. Gossard, and D. D. Awschalom, Science **306**, 1910 (2004).
[4] S. A. Wolf, D. D. Awschalom, R. A. Buhrman, J. M. Daughton, S. von Molnar, M. L. Roukes, A. Y. Chtchelkanova, and D. M. Treger, Science **294**, 1488 (2001).
[5] V. K. Kalevich and V. L. Korenev, Pis'ma v ZhETF **57**, 557 (1993) [JETP Lett. **57**, 571 (1993)].
[6] S. Hallstein, M. Oestreich, W. W. Ruhle, and K. Kohler, in *Proceedings of 12th International Conference High Magnetic Fields in the Physics of Semiconductors* (World Scientific, Singapore, 1996), p. 593.
[7] P. S. Eldridge, J. Hubner, S. Oertel, R. T. Harley, M. Henini, and M. Oestreich, Phys. Rev. B **83**, 041301(R) (2011).
[8] E. L. Ivchenko and A. A. Kiselev, Sov. Phys. Semicond. **26**, 827 (1992).
[9] P. Pfeffer and W. Zawadzki, Phys. Rev. B **74**, 233303 (2006).
[10] A. P. Heberle, W. W. Ruhle, and K. Ploog, Phys. Rev. Lett. **72**, 3887 (1994).
[11] A. Malinowski and R. T. Harley, Phys. Rev. B **62**, 2051 (2000).
[12] Yu. A. Nefyodov, A. A. Fortunatov, A. V. Shchepetilnikov, and I. V. Kukushkin, Pis'ma v ZhETF **91**, 385 (2010) [JETP Lett. **91**, 357 (2010)].
[13] Yu. A. Nefyodov, A. V. Shchepetilnikov, I. V. Kukushkin, W. Dietsche, and S. Schmult, Phys. Rev. B **83**, 041307(R) (2011).
[14] M. Dobers, K. von Klitzing, and G. Weimann, Phys. Rev. B **38**, 5453 (1988).
[15] D. Stein, K. von Klitzing, and G. Weimann, Phys. Rev. Lett. **51**, 130 (1983).
[16] A. Berg, M. Dobers, P. R. Gerhardts, and K. von Klitzing, Phys. Rev. Lett. **64**, 2563 (1990).
[17] N. Nestle, G. Denninger, M. Vidal, C. Weinzierl, K. Brunner, K. Eberl, and K. von Klitzing, Phys. Rev. B **56**, R4359 (1997).
[18] E. Abrahams, Physica E **3**, 69 (1998).
[19] G. Lommer, F. Malcher, and U. Rössler, Phys. Rev. B **32**, 6965 (1985).